Eur. Phys. J. B **37**, 425–432 (2004)
DOI: 10.1140/epjb/e2004-00077-1

THE EUROPEAN PHYSICAL JOURNAL B

^{207}Pb MAS NMR and conductivity identified anomalous phase transition in nanostructured PbF_2

P. Thangadurai[1], S. Ramasamy[1,a], and P.T. Manoharan[2,b]

[1] Department of Nuclear Physics, University of Madras, Guindy Campus, Chennai 600 025, India
[2] Department of Chemistry, Regional Sophisticated Instrumentation Centre, Indian Institute of Technology Madras, Chennai 600 036, India

Received 17 May 2003 / Received in final form 1st February 2004
Published online 9 April 2004 –

Abstract. Lead fluoride, a superionic conductor was prepared in its nanostructured form by Inert Gas Condensation Technique (IGCT) using an Ultra High Vacuum (UHV) chamber. The average grain size was found to be in the range 9 to 43 nm. The existence of mixed phases (α and β-PbF_2) was identified using XRD. Solid state ^{207}Pb MAS NMR was carried to average out the dipolar interaction and the resultant isotropic peaks were assigned to the corresponding phases. At high spinning frequencies, one isotropic peak emerged from the contribution of the grain boundary region. The relative intensity of this peak is reduced as the grain size is increased, independent of the concentration of the phases. This is related to the fact that the volume fraction of grain boundary atoms in nanostructured materials increases with the reduction of grain size. The width of the NMR resonance peak is found to be reduced as the grain size goes down. The structural phase transformations were identified at two different temperature regions. The first phase transformation from β to α phase in the annealing temperature range 573 K to 623 K is attributed to some anomalies related to the material microstructure and this has not been reported in earlier literatures. The second phase transformation from α to β in the temperature range 623 K to 673 K is similar to the already reported transformation. Electrical conductivity σ, of the samples was obtained from the complex impedance spectroscopy studies. Conduction species was identified as F^- ion through anion vacancies. The magnitude of the conductivity varied according to the dominant phase available when the grain size is higher. But at lower grain sizes below 20 nm, it shows enhanced conductivity that is attributed to the grain size effect. The NMR and conductivity data have jointly supported the anomalous phase transition at the annealing temperature of 623 K.

PACS. 72.60.+g Mixed conductivity and conductivity transitions – 61.10.Nz X-ray diffraction – 76.60.-k Nuclear magnetic resonance and relaxation – 76.60.Cq Chemical and Knight shifts

1 Introduction

Nanostructured materials have received much attention in recent research of science and technology because of their different physical and chemical properties. Many of their properties were found to be different when their grain size is reduced [1]. Lead fluoride (PbF_2) is a superionic conductor with high ionic conductivity due to large number of available Frenkel defects and its fluorine-ion disorder [2]. It exists in two allotropic forms, orthorhombic (α-PbF_2) and cubic (β-PbF_2) phases. These two phases can be converted from one to the other by applying pressure or by suitable heat treatment. The temperature and pressure dependence of the ionic conductivity and dielectric properties of both phases have been studied by Samara [3,4]. It can be used as an efficient electrolyte [5,6] in solid state batteries. Solid fluoride electrolytes (like CaF_2 and PbF_2) have also been used in chemical sensors because of their high ionic conductivity with negligible electronic conductivity [7]. The electrical properties of both α and β-PbF_2 have been studied rigorously by many authors [8–11]. Thermal properties of PbF_2 at low temperatures have been studied by measuring its thermal expansion coefficients [12]. Radiation resistivity measurements on PbF_2 have been done by Kozma et al. [13]. It can also be used as a Cherenkov radiator for electromagnetic calorimetry [14].

Nuclear magnetic resonance (NMR) is a powerful tool to study the local environment of NMR active nuclei. Developments such as magic angle spinning (MAS) improve the quality of the solid state NMR spectrum by spinning the sample at the magic angle $54°44'$ with respect to the applied field B_0 and the nuclei ^{207}Pb is a viable candidate for the NMR studies because of its following parameters: spin 1/2; gyromagnetic ratio $\gamma = 5.568 \times 10^{-7}$ rad T^{-1};

[a] e-mail: sinna_ramasamy@yahoo.com
[b] Honorary Professor, JNCASR, Bangalore

natural abundance 26% and its high atomic number. More electrons around the nucleus make it more sensitive to the chemical shift of the ^{207}Pb environment. ^{207}Pb NMR has been applied to many lead containing compounds [15,16] and the correlation between chemical shift and structure has been investigated. ^{19}F MAS NMR has been applied to PbF_2 to study the ^{19}F ion mobility by carrying out experiments at various temperatures [8,17]. Other structural investigations have also been performed using ^{207}Pb MAS NMR to correlate empirically the chemical shift with the structure of solids through coordination number or bond length [18]. Cross polarization magic angle spinning (CP-MAS) ^{207}Pb NMR with ^{19}F decoupling [19] has been used to correlate isotropic chemical shift with the number of next nearest neighbours. As far as nanostructured materials are concerned, some of the metals such as Cu [20] and Ag [21] were studied by using static solid state NMR and a resonance peak was observed that was attributed to the grain boundary. In this study we have performed solid state ^{207}Pb MAS NMR on the nanostructured mixed phase of PbF_2 with different grain sizes. We have made an attempt to interpret the spectrum on the basis of the phases present and the grain size. Also we have reported an anomalous phase transformation from β to α phase when the sample was annealed at 623 K. To the best of our knowledge this is the first time this measurement has been made on nanostructured PbF_2 although many have worked on bulk PbF_2 [2–5]. Electrical conductivity results obtained from complex impedance spectroscopy technique were found to show similar trend as the NMR results to support the anomalous transformation from β to α phase on annealing the as-prepared sample at 623 K.

2 Experimental procedure

The nanostructured lead fluoride (PbF_2) samples used in this study were prepared by inert gas condensation method, one of the pioneer methods used for the preparation of nanostructured materials. The precursor material used was PbF_2 bought from M/s. Sigma Chemicals Company, Inc., USA with the purity of 99.99%. The precursor was loaded in a molybdenum boat and kept in an ultra high vacuum chamber which was evacuated down to 4.1×10^{-8} torr. The partial pressures of residual gases were checked by the residual gas analyzer and the mass spectrum for six predominant gases is given in Figure 1. The mass spectrum given in Figure 1 was taken using the VacScan residual gas analyzer from Spectra Sensor Tech Ltd., UK. The chamber was filled with He gas up to a pressure of 0.5 mbar (0.38 torr) as a carrier gas. Then the sample was evaporated by resistive heating using a high current transformer. The evaporated vapour forms nanoclusters due to the pressure of helium. These clusters were deposited on a cold finger kept at 77 K due to the convection current set up between the cold finger and the boat, because of the difference in temperature. After complete evaporation, He was evacuated down to 5×10^{-7} torr. Then the deposited powder was scraped, collected and stored under vacuum for further analysis. The

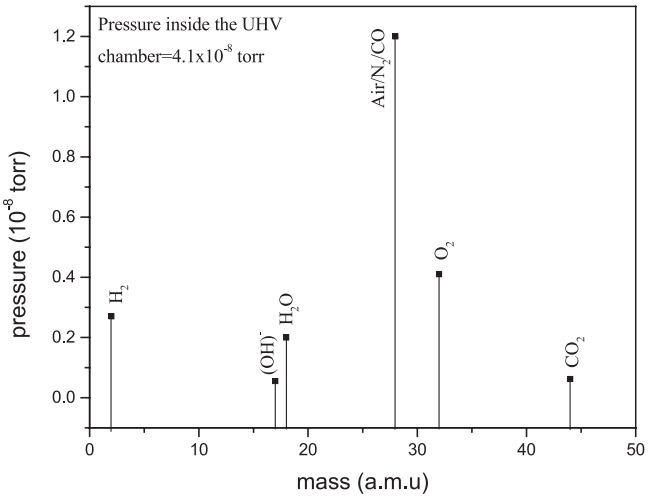

Fig. 1. Mass spectrum of residual gases (six predominant gases) available in the UHV chamber before the evaporation of PbF_2. Pressure inside the chamber while taking this spectrum is 4.1×10^{-8} torr.

as-synthesized samples were annealed at different temperatures for 1 hour under a vacuum of the order of 10^{-5} torr so as to obtain various grain sizes and to remove strain from the material. Six such samples were used in our study.

The structural phases of PbF_2 were identified by the X-ray diffraction (XRD) pattern obtained using a X-ray diffractometer manufactured by Siefert Inc., Germany. The grain size calculations were done using the full width at half maximum (FWHM) of the XRD peak in the modified Scherrer formula [22], which takes care of instrumental resolution and widening of the peaks due to residual stress. ^{207}Pb MAS NMR measurements for the samples were done on a BRUKER DRX500 instrument with an operating frequency of 104.2656 MHz. The samples were packed into a 4 mm zirconia rotor and spun at different speeds. A spectral width and a pulse width were 1 MHz and 3 μsec ($\sim$45° flip angle) respectively. The signals were collected with 1 second recycle delay time by applying a simple one pulse in a broadband 4 mm CP/MAS probe. The raw data were subjected to exponential multiplication with a line broadening of 100 Hz prior to Fourier Transformation. Three sets of NMR data have been taken for each sample with the spinning frequencies 4 kHz, 10 kHz and 12.5 kHz (i.e., the spinning frequency of the 4 mm zirconia rotor).

The powder samples were isostatically pressed into discs whose diameter and thickness varied between 8.20 to 8.27 mm and 0.36 and 0.56 mm respectively. Silver electrodes were used. Impedance measurements were carried out using a Solartron 1260 Impedance/Gain Phase analyzer as a function of frequency in the range between 1 Hz to 10 MHz on all the pressed samples in the temperature range from 300 K to 523 K (measured under vacuum of the order of 10^{-5} torr). Data acquisitions were automated by interfacing the impedance analyzer with the computer. The impedance data plotted in a complex impedance

plane was fitted with a Non-Linear Least Square (NLLS) method to get resistance. This resistance has been converted into conductivity using the formula $\rho = RA/l$, where R is the resistance, A is the area of cross section and l is the thickness of the sample disc. For our discussions, conductivity values measured at 373 K alone were considered.

3 Results and discussion

For convenience, the samples as-synthesized and those annealed at temperatures 423, 473, 573, 623 and 673 K for 1h under vacuum are labeled as PbF2-As, PbF2-423, PbF2-473, PbF2-573, PbF2-623 and PbF2-673 respectively. XRD patterns of the nanostructured PbF_2 with various grain sizes are given in Figure 2. Along with the sample label the corresponding grain size is also given in bracket against each pattern. It is found that the grain growth is faster even at low annealing temperatures such as 423 K and 473 K.

From the XRD patterns it is observed that the PbF2-As, PbF2-423 and PbF2-623 contain high concentrations of α-PbF_2 mixed with β-PbF_2. It is already reported that the conversion of α phase to β phase can be achieved by annealing the former at 673 K for 1 h in an inert atmosphere [8]. The interconversion between α and β phases is very sensitive to pressure and temperature and this has been thoroughly studied by Samara [3,4]. Samara has reported in his paper that the α phase can be achieved by applying a pressure of 4 kbar on the β phase sample and the latter could be recovered by heating the former at about 610 K till to achieve a sample without residual stress. Here we do not study the role of pressure and hence the metastability of the sample with temperature alone should be considered very carefully. In the nanocrystalline form we could get only a mixed phase of PbF_2 even at room temperature. However, the samples PbF2-473, PbF2-573 and PbF2-673 contain much higher concentration of β-PbF_2 with one weakly intense peak of the α phase. These samples can be referred here as pure β-PbF_2. The structural data obtained from XRD are comparable to the earlier reports [23–25]. Ehm et al. [23] have observed the single phase of α-PbF_2 by applying a pressure of 3.8 GPa. Nagai et al. have obtained the mixed and single phases with the starting powder and the heat treated sample respectively in pure [24] and composite [25] PbF_2.

It is interesting to note that when the annealing temperature was raised from 573 K to 623 K, the β phase is transformed into more intense α phase. The reverse is observed by raising the annealing temperature further to 673 K. It is reported previously [3] that the α phase can be transformed completely to β by heat treatment at ∼610 K for appropriate time and this phase is stable unless it is disturbed by the high pressure. In contradiction to the earlier observations, around the same annealing temperature range, we observed the β to α transformation. This anomalous phase transformation may be due to some microstructural re-organization such as grain orientation or

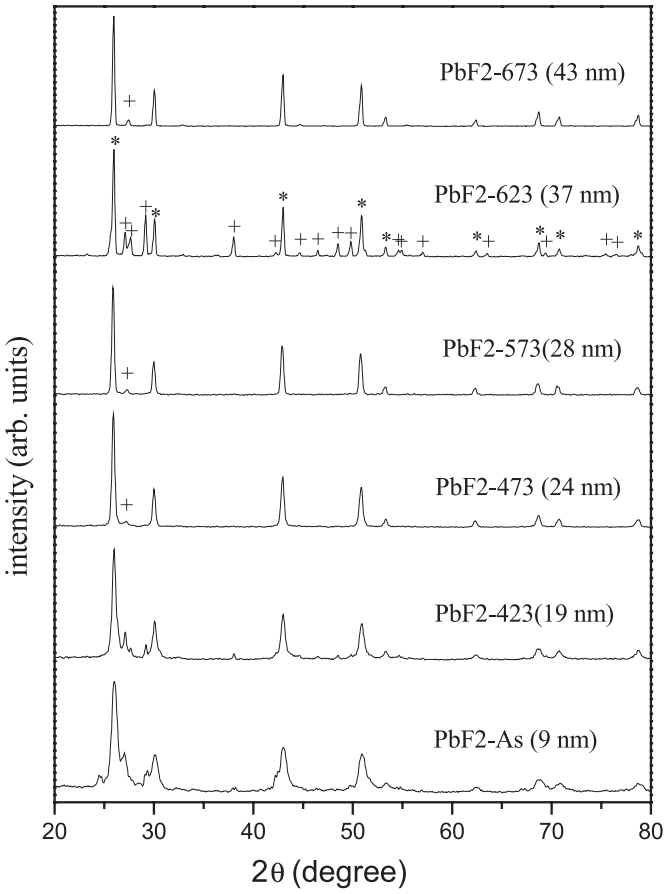

Fig. 2. XRD patterns for nanostructured PbF_2 with different annealing temperatures and grain sizes. Along with the sample label, the grain size is also given within the bracket against the corresponding pattern (* refers to β-PbF_2; + refers to α-PbF_2). Isochronal annealing was done under vacuum for 1 h.

grain size induced structural change during thermal treatment. This phase formation may also be the crystallization of the amorphous phase present in the grain boundary region. This anomalous β to α phase transition will be discussed in detail using the NMR and ionic conductivity measurements. The relative quantities of both the phases present in each sample were calculated from the relative intensities of the corresponding phases in the XRD pattern [26]. This data will be later compared with the same obtained from the NMR spectra.

The ^{207}Pb MAS NMR spectra of all the samples of nanostructured PbF_2 taken at 4 kHz, 10 kHz and 12.5 kHz are given in Figures 3a–f. Due to the large polarization of the electrons surrounding the ^{207}Pb nuclei, its observed chemical shift is very high with respect to the secondary reference namely $Pb(NO_3)_2$ which in turn is referenced to the standard reference for lead NMR, tetramethyl lead ($Pb(CH_3)_4$) [18]. In general, the NMR spectral lines were found to be broad. We can attribute this overall broadening to two possibilities: a) incomplete averaging of the strong dipolar coupling with the neighbouring atoms at these frequencies; b) disorder inherent to the lattice [20,21]. In nanocrystalline solids the grain boundaries

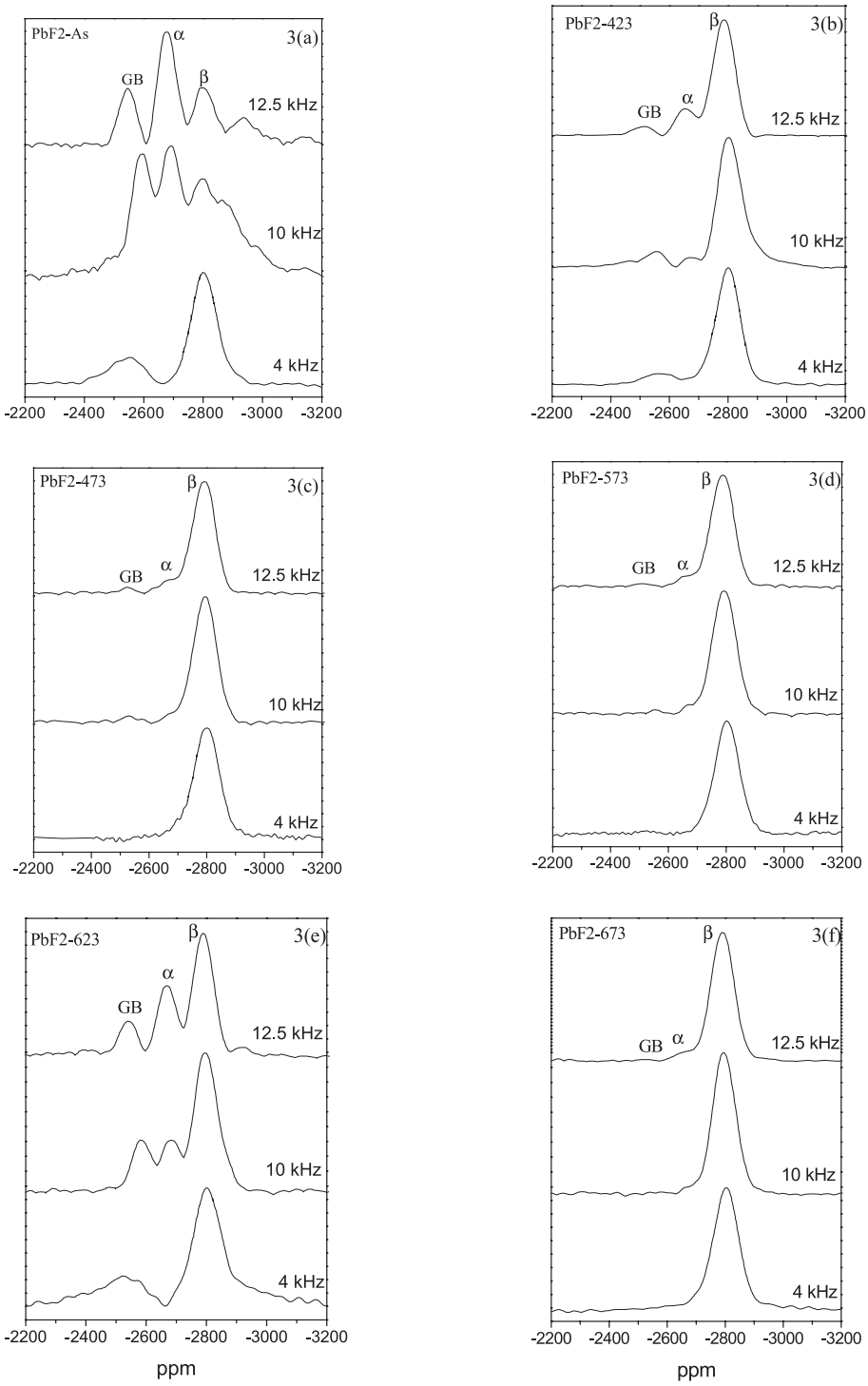

Fig. 3. (a–f). ^{207}Pb MAS NMR spectra of nanostructured PbF_2. Spinning frequencies are given near the corresponding spectrum. Sample label is given at the top left corner of each figure.

contain disordered atoms [1]. This disorder may contribute to the additional line broadening. As the spinning frequency of the rotor increases there is a slight shift observed in the isotropic chemical shift due to the effect of increase of temperature inside the MAS rotor caused by frictional heating [18,19] even though all the NMR measurements were carried out at room temperature.

All the spectra have become better resolved as the spinning frequency increases as a consequence of reduced dipolar interaction. All the spectra were fitted with the Peakfit, a grapher software. Invariably all the spectra could be fitted with three Gaussian components. The distinction between the α and β phases are identified on the basis of the signal intensity [18] corresponding to the

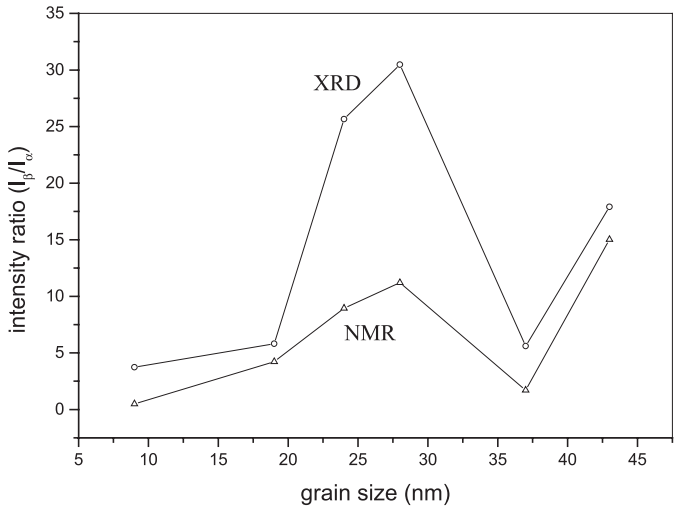

Fig. 4. Relative intensity of β-PbF_2 to α-PbF_2 as calculated from the peak amplitudes of the NMR and XRD spectra for various grain sizes (lines are guide to eyes).

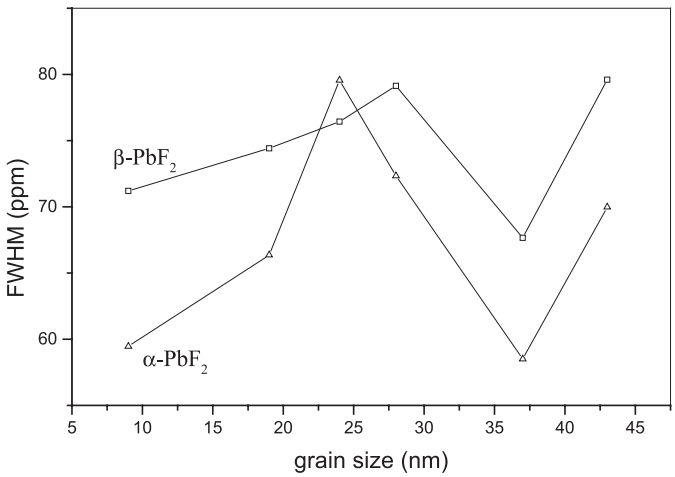

Fig. 5. Variation of FWHM for α and β phases of the nanostructured PbF_2 as calculated from NMR data (lines are guide to eyes).

relative concentration of the phases present in the sample. The isotropic peak positions corresponding to the α-PbF_2, β-PbF_2 and grain boundary components are noted in the figures by the symbols α, β and GB respectively. Other than PbF2-As all the other samples show the intense β-PbF_2 resonance peak in exact agreement with the results observed from the XRD analysis. The concentration of β-PbF_2 increases as the annealing temperature varied up to 573 K. With the annealing temperature 623 K, α-PbF_2 appears again from the β-PbF_2 phase. This is shown in the Figure 3e which is the NMR spectra of PbF2-623, and contains three peaks corresponding to both the phases and the grain boundary component. The results observed from XRD for this sample is in exact correspondence with the NMR results. The relative intensities of the β-PbF_2 to α-PbF_2 observed from NMR and its comparison with the intensity ratio observed from XRD are given in Figure 4. A similar trend from these two measurements is easily seen. In most experiments, the α phase is found to appear only at higher spinning frequencies. This could be due to the presence of large chemical shift anisotropy at the ^{207}Pb nucleus for the orthorhombic α phase as compared to the almost nonexistence of this factor in the cubic β phase. This contribution could have added to other broadening mechanisms such as dipolar in the α phase and hence higher spinning frequencies could become a necessity for a better resolution of this phase.

Figure 5 gives the full width at half maximum (FWHM) of both the α and β phases obtained from the NMR data as a function of grain size (i.e. as a function of FWHM of the XRD peaks since the grain size is proportional to the inverse of FWHM). As far as the β-PbF_2 phase is concerned there is a regular increase in the width with the increase in the grain size. But in the sample PbF2-623, a sharp decrease is observed and this corresponds to the phase conversion from β to α during annealing of β-PbF_2 at 623 K for 1 h. At this temperature the sample goes from β phase to the mixed phase with a higher intensity for the α phase. This may be correlated to the ordering of the grain boundary atoms. As the grains are already dominated by the β phase atoms, the probability that the grain boundary atoms participate in the α phase formation is comparatively greater. This will increase additional ordering in the lattice and hence the lattice strains due to the grain boundary atoms will be reduced. This is like the segregation of solute in grain boundaries; viz. α phase as a secondary phase in grain boundaries. It is similar to the observations in many ionic conductors like ZrO_2 [27]. This lattice ordering (*vide supra*), in turn, is responsible for the reduced NMR linewidth. Also this may lead to a variation in conductivity as discussed later. Again the phase conversion in PbF2-623 to the β phase is the one corresponding to the usually observed phase transformation [3]. Similar linewidth behaviour was observed also for α-PbF_2. In nanostructured metals, as studied by Suits et al. [20,21] the FWHM of NMR line increases as the grain size is decreased. In metals the contribution to the peak width is predominantly from the paramagnetic electrons. In our case, no paramagnetic contribution is available and hence it behaves in a reverse way.

Figure 6 shows the isotropic chemical shift (δ_{iso}) for the α and β phases of the nanostructured PbF_2. Isotropic chemical shift is observed to be larger for the α-PbF_2 than for the β-PbF_2, which is in good agreement with the results already reported [19]. The chemical shift for the α and β phases are reported as -2667 ± 2 ppm [18] and -2793 ± 1 [19] respectively, relative to $Pb(CH_3)_4$. The main difference between the two phases of the PbF_2 phases is that the Pb^{2+} ion is 9-fold coordinated in α-PbF_2 with the mean Pb^{2+}-F^- distance 2.770 Å and 8-fold coordinated in β-PbF_2 with the Pb^{2+}-F^- distance 2.567 Å [19]. The interatomic distance D is 0.2 Å less in β-PbF_2 than in α-PbF_2 providing a higher electron density around Pb^{2+} making every Pb-F bond contributing to greater shielding and hence larger chemical shift. The δ_{iso} for the β-PbF_2

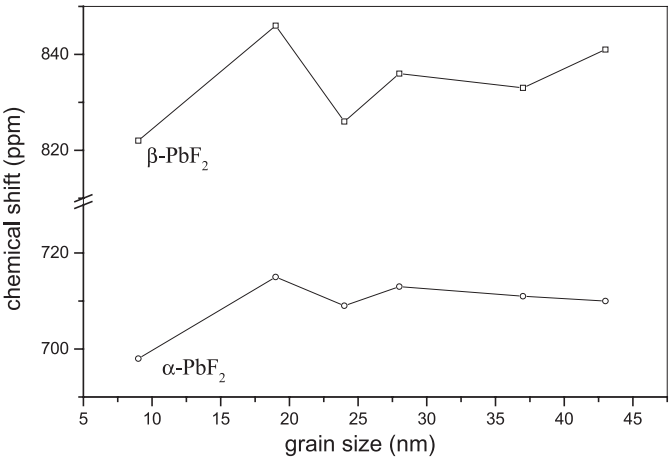

Fig. 6. Isotropic chemical shift against grain size for both the phases of nanostructured PbF_2 (lines are guide to eyes).

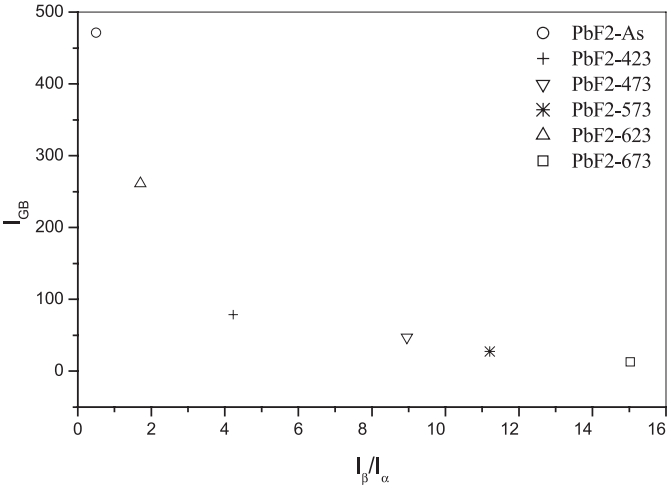

Fig. 7. Intensity of the resonance peak of the grain boundary against the intensity ratio of β to α (I_β/I_α) phases of PbF_2 for the samples with different grain size.

in Figure 6 shows slight irregular variation as a function of grain size and the variation is within 3%. Therefore this variation could not be attributed to the variation of grain size. A similar observation is made in the case of α-PbF_2 also.

Figure 7 shows the NMR peak intensity attributed to the contribution from the grain boundary (I_{GB}) of the nanostructured PbF_2 against the relative intensity of β to α (I_β/I_α) for various grain sizes. The importance of this peak is that this shows the existence of large amount of grain boundary ions/molecules in the nanostructured materials and when the grain size increases the number density of ions/molecules residing in the grain boundary will be reduced. From the figure it is apparent that the relative amplitude of the resonance peak from the grain boundary is reduced with the increase in I_β/I_α (i.e. with the grain size). The sample PbF2-623 alone shows the sudden increase in the grain boundary intensity I_{GB}. This increase is obvious due to the phase transition from β-PbF_2 to α-PbF_2 at annealing temperature of 623 K for 1 h and

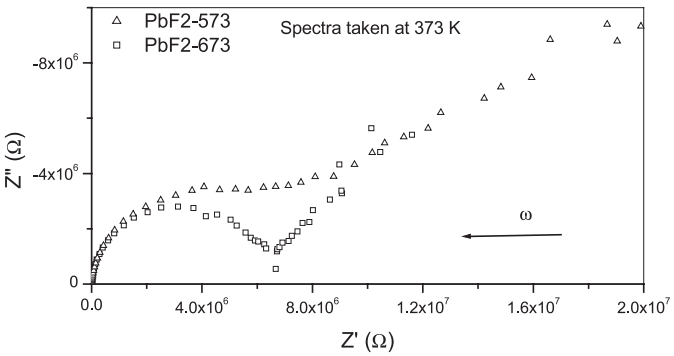

Fig. 8. Typical impedance spectra for the nanostructured PbF_2 samples PbF_2-573 and PbF_2-673. The spectra were taken at 373 K.

the co-existence of both the phases which leads to the availability of more interfaces. Because of the co-existence of both the phases in almost equal amounts, the strength of their interfacial component signifies the problem and its effect is added to the grain boundary component and hence the intensity shoots up. In the sample PbF2-673, whose grain size is 43 nm, the intensity of this peak almost becomes zero. From this observation, we can infer the existence of large fraction of Pb^{2+} ions in the grain boundaries in nanostructured PbF_2 with different atomic ordering compared to the grains.

Figure 8 shows the typical impedance spectra for two samples of nanocrystalline PbF_2 (PbF2-573 and PbF2-673) measured at 373 K under vacuum. The similar type of spectra was obtained for the other samples also and they are not shown here. The depressed semicircle in the impedance spectra was fitted with non-linear least square fit to get the resistance. This resistance values were converted into d.c. conductivity by multiplying them with the proper geometrical factors of the corresponding sample. A lower frequency rise in the tail corresponds to the surface charge polarization between the electrode-electrolyte of the cell assembly. We have obtained the semicircular arc whose center is slightly shifted down to the real axis Z'. This shows non-Debye type of relaxation in the sample with distribution of relaxation times [28]. Usually in impedance spectra, three such semicircular arcs are expected. Arcs at high, middle and low frequency regions are correlated to the contribution from grain (bulk or lattice), grain boundary and electrode-electrolyte interface effect respectively. In our case we have observed only one semicircular arc in the high frequency region and a continuous raise in the low frequency region corresponding to the electrode-electrolyte effect. The capacitance values of all the samples have been calculated and they are found to be in the range from 30 to 37 pF. Capacitance values calculated from the geometrical factors of the samples were also in range 0.85 to 1.35 pF. The presence of a single arc would mean one or more of the following possibilities: (i) there is no grain boundary (highly conductive grain boundaries); (ii) the time constants for both the processes are equal; (iii) the grain interior are so small as to be imperceptible [29]. Here we have highly conductive grain

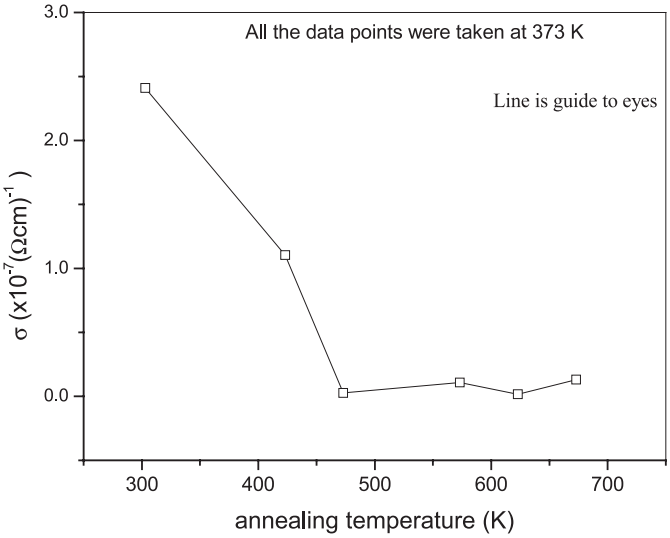

Fig. 9. Variation of electrical conductivity of nanostructured PbF_2 with the annealing temperature (grain size). The data points were measured at 373 K.

boundary as discussed later. Also, the facts that the arc is present in the high frequency region [30] and the capacitance value is around that of the grain interior (for grain boundary it is of the order of nF) [31] allow us to conclude that the semicircular arc originates from grain interior.

Figure 9 shows the variation of d.c. electrical conductivity as a function of annealing temperature (i.e., grain size). Some authors [27] have compared the single grain boundary conductivities of the nanocrystalline ZrO_2, a good ionic conductor, with impurities in the grain boundary using specific grain boundary conductivity. Our observation of a single arc corresponding to grain safely rules out the comparison of specific grain boundary contributions.

We observed a maximum conductivity for the lowest grain sized sample (PbF2-As); the conductivity also decreases with the increase in grain size up to 24 nm (PbF2-473). Thereafter there is a slight increase in the conductivity in the 28 nm sample (PbF2-573). For the 34 nm sample (PbF2-623), there is a slight fall in the conductivity and this variation is very important since it is a supportive evidence for the observed anomalous β to α phase transition. For the sample with 43 nm again we found a significant increase in conductivity. For lower grain sized samples, the higher value of conductivity is attributed to the grain size effect and the value of the same for the higher grain sized samples varies with the respect to the phases available in the samples. We know that PbF_2 is a superionic conductor and the conduction is through F^- ion vacancies [33], interstitial anions/ Frenkel defects [9]. At low temperatures, the conduction of F^- ion takes place through the anion vacancies by means of hopping mechanism. But at higher temperatures between 700 K and 800 K, F^- will have the diffuse transition due to the disordering of the F^- ion sublattice, this phenomenon being referred to as sublattice melting. Hence at this range, F^- ions have a continuous motion which leads to enormous conductivity, this state being superionic [3].

Bonne and Schoonman [32] have studied different stages of conductions in PbF_2 as a function of temperature. At low temperature region (between 300 and 500 K, it is said to be the second stage in [3]), they have determined that the conduction is purely due to F^- ion vacancies than by F^- ion interstitials. The activation energies we obtained from the Arrhenius plot (for the temperature range from 300 to 500 K) are in the range from 0.56 to 0.71 eV that agree well with their data for this stage II (activation energy from their data is 0.67 eV). According to this discussion, the conduction in our samples is mainly due to F^- ion vacancies in this measuring temperature range.

As the grain size goes down, number of defects formed in the grain boundary region and F^- ion finds its easy path through the grain boundary and consequently, the conductivity becomes higher. Even though the two samples PbF2-As and PbF2-423 contain a less conducting α phase (than the β phase) [34] to reasonable quantity, the conductivity is more and it is attributed to the grain size effect. After 24 nm, we could not find the grain size effect. The variation of conductivity is dominated by the available phases. For PbF2-473 to PbF2-573, the sample becomes almost pure β phase and hence we find the increase in conductivity. Then the sample PbF2-623 shows the fall in conductivity because of the new phase formation (α-phase) at this annealing temperature (623 K) and this α is less conducting phase [34]. As discussed earlier, ordering in the grain boundary leads to formation of α phase in the grain boundary region. Thus the total conductivity goes down. This is observed here as a fall in conductivity in PbF2-623 sample. The sample PbF2-673 is in β phase and shows the conductivity of the same order as PbF2-573 which also contains only the high conducting β phase of PbF_2. In general, the grain size dominates the conductivity when the former is low but in higher grain sized samples, the phase is the dominating factor. This result is well in agreement with the XRD and NMR results which showed the phase transition from β to α at the annealing temperature, 623 K.

4 Conclusion

The nanostructured PbF_2 was prepared using the inert gas condensation technique in an indigenously developed UHV chamber. The mixed phases of PbF_2 were obtained and the structural phase transformations were identified by using XRD. The annealed samples at different temperatures show a very high concentration of β phase. XRD patterns in annealed samples showed an anomalous β to α phase transition for the sample annealed at 623 K. From ^{207}Pb MAS NMR, the linewidth is found to decrease with the reduction of grain size. Isotropic chemical shifts were assigned to the α, β and the grain boundary components of the nanostructured PbF_2. The grain boundary component of this nanostructured materials implies different atomic ordering in the grain boundary compared to

the grains. Electrical conductivity study also reveals the anomalous phase transformation from β to α due to the microstructural reorganization of grain boundary atoms at the annealing temperature, 623 K and the conduction took place by F^- ions through anion vacancies. For lower grain sizes, the conductivity depends on the grain size but for the higher grain sizes, it is dominated by the structural phases of the material.

The authors are thankful to Dr. Ganapathy and Dr. Rajamohanan, NCL, Pune, India for their help in taking NMR measurements and Dr. A. Chandra Bose, NIMS, Japan for his help during sample preparation. Constant encouragement from Prof. P.R. Subramanian is kindly acknowledged. The support from the DST, UGC-SAP and COSIST programmes is also acknowledged. One of the authors PT acknowledges the financial support from the CSIR-India by the award of SRF (9/115(565)/2002-EMR-I). The author PTM thanks the DST, Government of India for a scheme (SP/S-1/F-18/2000).

References

1. H. Gleiter, Prog. Mater. Sci. **33**, 223 (1989)
2. C.E. Derrington, A. Navrotsky, M. O'Keeffe, Solid State Commun. **18**, 47 (1976)
3. G.A. Samara, J. Phys. Chem. Solids **40**, 509 (1979)
4. G.A. Samara, Phys. Rev. B **13**, 4529 (1976)
5. J.H. Kennedy, R. Miles, J. Hunter, J. Electrochem. Soc.: Electrochem. Sci. Tech. **120**, 1441 (1973)
6. N. Egashira, H. Kokado, Jpn J. Appl. Phys. **25**, L462 (1986)
7. J.W. Fergus, Sensors and Actuators B **42**, 119 (1997)
8. J. Schoonman, L.B. Ebert, C.H. Hsieh, R.A. Huggins, J. Appl. Phys. **46**, 2873 (1975)
9. C.E. Derrington, M. O'Keeffe, Nature **246**, 44 (1973)
10. C.C. Liang, A.V. Joshi, J. Electrochem. Soc.: Electrochem. Sci. Tech. **122**, 466 (1975)
11. J. Schoonman, G.A. Korteweg, R.W. Bonne, Solid State Commun. **16**, 9 (1975)
12. G.K. White, J. Phys. C **13**, 4905 (1980)
13. P. Kozma, R. Bajgar, P. Kozma Jr, Nucl. Inst. Meth. Phys. Res. A **484**, 149 (2002)
14. D.F. Anderson, M. Kobayashi, C.L. Woody, Y. Yoshimura, Nucl. Inst. Meth. Phys. Res. A **290**, 385 (1990)
15. Y.-S. Kye, S. Connolly, B. Herreros, G.S. Harbison, Main Group Metal Compounds **22**, 373 (1999)
16. H.G. Niessen, M. Van Buskirk, C. Dybowski, D.R. Corbin, J.A. Reimer, A.T. Bell, J. Phys. Chem. B **105**, 2945 (2001)
17. F. Wang, C.P. Grey, J. Am. Chem. Soc. **120**, 970 (1998)
18. F. Fayon, I. Farnan, C. Bessada, J. Coutures, D. Massiot, J.P. Coutures, J. Am. Chem. Soc. **119**, 6837 (1997)
19. B. Bureau, G. Silly, J.Y. Buzaré, Solid State NMR **15**, 79 (1999)
20. B.H. Suits, M. Meng, R.W. Siegel, Y.X. Liao, J. Mater. Res. **9**, 336 (1994)
21. B.H. Suits, R.W. Siegel, Y.X. Liao, Nanostruct. Mater. **2**, 597 (1993)
22. B.D. Cullity, in *Elements of X-ray Diffraction* (Addison-Wesley, 1977), p. 81
23. L. Ehm, K. Knorr, F. Mädler, H. Voigtländer, E. Busetto, A. Cassetta, A. Lausi, B. Winkler, J. Phys. Chem. Solids **64**, 919 (2003)
24. M. Nagai, T. Kushida, T. Nishino, Solid State Ionics **62**, 151 (1993)
25. M. Nagai, T. Nishino, Solid State Ionics **99**, 221 (1997)
26. A. Meyer, J. Ten Eicken, O.V. Glumov, W. Gunsser, M. Karus, I.V. Murin, Rad. Effects: Defects in Solids **137**, 147 (1995)
27. M. Aoki, Y.-M. Chiang, I. Kosacki, L.J.R. Lee, H. Tuller, Y. Liu, J. Am. Ceram. Soc. **79**, 1169 (1996)
28. A.K. Jonscher, J.M. Réau, J. Mater. Res. **13**, 563 (1978)
29. J. Lee, J.-H. Hwang, J.J. Mashek, J.O. Manon, A.E. Miller, R.W. Siegel, J. Mater. Res. **9**, 2295 (1995)
30. R.N. Viswanath, S.N. Ramasamy, Mater. Trans. **42**, 2601 (2001)
31. A. Chandra Bose, Ph.D. thesis, University of Madras, India, p. 115 (2002)
32. R.W. Bonne, J. Schoonman, J. Electrochem. Soc.: Electrochem. Sci. Tech. **124**, 28 (1977)
33. J.H. Kennedy, R.C. Miles, J. Electrochem. Soc.: Solid State Sci. Tech. **123**, 47 (1976)
34. G.A. Samara, Ferroelectrics **17**, 357 (1977)